

Identifying Spatial Patterns of Recovery and Abandonment in the Post-Katrina Holy Cross Neighborhood of New Orleans

Andrew Curtis , Dominique Duval-Diop & Jenny Novak

To cite this article: Andrew Curtis , Dominique Duval-Diop & Jenny Novak (2010) Identifying Spatial Patterns of Recovery and Abandonment in the Post-Katrina Holy Cross Neighborhood of New Orleans, *Cartography and Geographic Information Science*, 37:1, 45-56, DOI: [10.1559/152304010790588043](https://doi.org/10.1559/152304010790588043)

To link to this article: <https://doi.org/10.1559/152304010790588043>



Published online: 14 Mar 2013.



Submit your article to this journal 



Article views: 300



View related articles 



Citing articles: 10 View citing articles 

Identifying Spatial Patterns of Recovery and Abandonment in the Post-Katrina Holy Cross Neighborhood of New Orleans

Andrew Curtis, Dominique Duval-Diop, and Jenny Novak

ABSTRACT: The devastation caused by Hurricane Katrina is still being felt by many neighborhoods of New Orleans and along the Gulf Coast. As these communities struggle to recover, academia has been forced to acknowledge that there is little known or theorized about the spatial processes of recovery, especially at the fine scale. As a result this paper will investigate how post-disaster landscape characteristics can be extracted from spatial video data for neighborhoods of New Orleans. These will be turned into a statistical surface using analytical approaches more commonly applied in spatial epidemiology. Spatial patterns of abandonment and recovery will be identified that can be used as a basis for a next round of causative investigation. The paper finds that by using the spatial overlap of four different analyses involving two different data input locations and two filter sizes, the Holy Cross neighborhood of New Orleans does indeed reveal areas with higher rates of recovery, and continuing abandonment. However, even within these areas, spatial heterogeneity can be found. This paper uses Google Street View to mirror spatial video data collected in participatory collaborations with New Orleans community groups so that readers can replicate the methods presented here for other neighborhoods of New Orleans.

KEYWORDS: Hurricane Katrina, GIS, spatial video, neighborhood recovery

Introduction

In August and September 2005, Hurricanes Katrina and Rita (from this point on referred to as Katrina) made landfall, leaving in their wake massive loss of life, property, business, and community (Cefalu et al. 2006; Hartman and Squires 2006; Kunreuther 2006; Madrid et al. 2006). Unfortunately, as of the summer of 2009, many neighborhoods in Orleans and St Bernard Parish were still struggling to reestablish themselves, the few returnees being faced with multiple abandoned and overgrown properties, lost neighbors and churches (and therefore social support networks), and severely limited infrastructure (Holzer and Lerman 2006; Penner and Ferdinand 2009). This disaster has illustrated existing disparities between

communities in New Orleans, and how these social impediments also become hindrances to recovery (Vale and Campanella 2005; Bullard and Wright 2009). We should also acknowledge how little we understand about the recovery process from a *spatial perspective*. There have been few data-driven spatial analyses at the street and neighborhood scale of *who returns, why they return, and what patterns result*. This paper will not provide explanations or causations of the fine-scale processes involved but rather suggest a methodological framework needed to begin the discourse.

The Spatial Analysis of Recovery

Although post-disaster recovery has received attention by academics (Haas et al. 1977; Wright et al. 1979; Comerio 1998; Alesh et al. 2009), fine-scale spatial analysis of the processes involved has been lagging for a number of reasons, though mainly because data are not widely available (Duval-Diop and Rose 2008; Mills 2008). Utility or mail service delivery data and other proprietary data collected by contractors could provide spatial insight in some cases, but they are extremely hard to obtain, resulting in

Andrew Curtis, Jenny Novak, Department of Geography College of Letters, Arts and Sciences University of Southern California, Kaprielian Hall (KAP), Room 448B, 620 South Vermont Avenue, Los Angeles, California 90089-0255, Telephone: 213 740 0061, Fax 213 740 9687. E-mail: <ajcurtis@usc.edu> <wrye@usc.edu>. **Dominique Duval-Diop,** Former Senior Associate, PolicyLink, 1515 Poydras, Suite 105 New Orleans, Louisiana 70112. E-mail: <ddiop@consultfermina.com>.

difficulties in performing confirmatory analyses by researchers. Consequently, advances or insights cannot be built upon, or even translated to other locations. Other data, such as building permits hold more promise as an accessible point-level source for change. However, all of these data only tell one part of the return/abandonment story; they do not describe the visual impact on neighborhoods and the stress returnees have to deal with.

A second problem is the spatial scale at which data are available. There are some excellent data reporting bodies and warehouses associated with Katrina and New Orleans, such as the Greater New Orleans Community Data Center and the LSU Clearinghouse Cooperative (Mills et al. 2008). However they do not release fine-scale residential data for confidentiality reasons. Data released by zip code, by census enumeration unit (Liu and Plyer 2008), or even for an entire “neighborhood” such as the Lower 9th Ward have severe limitations (Duval-Diop et al. 2010; Grubesic et al. 2006), not least of which is that nuances in disaster exposure (e.g., depth of flooding) could be missed at the neighborhood scale. For example, zip code 70177 shown in Figure 1 contains parts of eight different, commonly referenced “neighborhoods,” including the Lower 9th Ward and Holy Cross, the subject of this paper (Curtis 2008). Not having fine-scale data is problematic as many of the local processes either impeding or promoting recovery work at the sub-neighborhood level (for example a church stimulating the recovery in the block surrounding it). It is therefore imperative to be able to analyze abandonment and recovery at a finer scale, ideally by home and street segment.

Also, in order to be an effective measure of neighborhood change, data must be collected during multiple time periods as recovery is longitudinal and not just cross-sectional. In order to develop a fine-scale spatial recovery theory, data need to

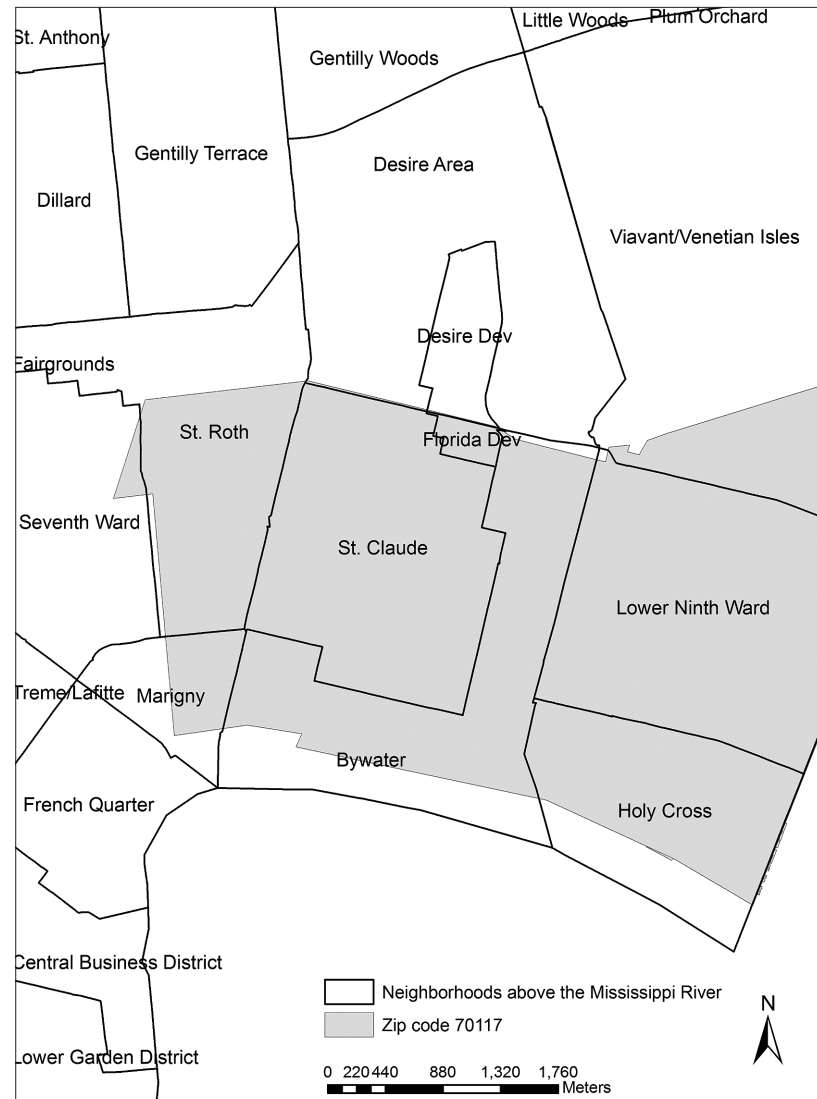


Figure 1. Neighborhoods of New Orleans. This map identifies several of the neighborhoods in proximity to Holy Cross, the subject of this paper. The boundary for Zip code 70117 is also displayed to show how inappropriate data available at this scale is for fine scale recovery analyses because of its spatial mismatch with neighborhood areas.

be available at an appropriate scale, for multiple time periods, and with easy accessibility for both researchers and community groups alike. This is not to say that other local area spatial analyses of recovery data are not warranted, even if they use propriety data or are for one time period. As previously mentioned, our understanding of the recovery process is limited, and any additional investigation that might reveal spatial patterns or trends would be welcome (Mills 2008).

Given this need for fine scale-spatial analyses of recovery data, our objectives in this paper are to:

1. Provide an effective template for encoding “recovery” data from collection / acquisition to a

- statistical surface suitable for analysis, and one that is transferable between neighborhoods and disasters; and
- 2. Use spatial analysis to identify area patterns with substantial abandonment and intra-neighborhood high rates of returnee re-occupancy.

The Need for Collecting Fine-Scale Recovery Data

Community groups are often able to describe the unevenness of recovery in their neighborhoods but are rarely able to support these observations with quantifiable analyses. To do this, data are needed which reflect fine-scale updates of the actual rebuilding progress. In other words, data which highlight the connection at a neighborhood level between city redevelopment efforts, state housing repair programs, and the actual rebuilding of homes on a city street. The number of properties which remain blighted or abandoned is a powerful means of assessing the actual progress on the ground, and the impact of slow recovery programs on neighborhood rebuilding. A map of blight or recovery would be a particularly useful tool for informing policymakers about recovery efforts, especially if it were to map data from multiple time periods for comparison.

If community groups are involved in data collection needed to generate such maps, then not only will the geographic scale and location be appropriate for their needs, but they will also be contributing directly to the recovery. Empowering communities in this way is imperative for their resilience (Richards and Dalbey 2006; Petersen et al. 2006). As an example of one such collaboration between Churches Supporting Churches (CSC) and the Department of Geography at the University of Southern California (USC), returnees were mapped at the individual property level in the Lower 9th Ward for the period 2007 to 2009. These data were also incorporated by PolicyLink into maps showing the rebuilding gap, i.e., the difference in dollar value between the compensation an owner has received and the amount required to fully rebuild.

Although there are different datasets available which can be used to capture residence-level recovery (and abandonment), such as postal delivery data or utility use, they are often hard to acquire by neighborhood associations. In addition, they may not capture visually the extent of blight on the street. For these reasons, data collected by the

CSC and USC team utilized spatially encoded video. There is considerable precedent for using visual assessments of the built environment, with videography previously being used by sociologists to rate observed incivilities in the built environment (Sampson and Raudenbush 1999), and Red Cross still uses visual damage assessment to code post-disaster buildings (Curtis et al. 2007).

The CSC/USC recovery assessment approach used multiple video cameras aboard a vehicle and synched to a global positioning system encoding a continuous coordinate stream onto the audio track of each tape. Cameras were placed around the vehicle, but they primarily captured the right and left sides of the street. After post-processing data were extracted into a GIS, either as points or attached to digitized building footprints (Curtis et al. 2009).

The data collection team involved a community representative providing a vehicle and a driver and selecting the route. The representative provided commentary on the landscape as it was videotaped. The neighborhood group thus had a major input on where data should be collected, and in the data collection process in general. The maps generated were used to identify abandonment, rebuilding and recovery, and, importantly, quantifiable scales of each. In addition other elements of the post-disaster landscape were extracted from the video, such as the amount of vegetation overgrowth, the continuing presence of search and rescue markings, visible signs of infrastructure disrepair (especially quality of roads), the state of physical anchors of social networks (e.g., local stores and churches), and whether abandoned buildings were secured or not. In some instances, data were used by external organizations assisting the neighborhood, such as PolicyLink, which combined the spatial video output with other information to help provide a more holistic assessment of community needs (Duval-Diop et al. 2010).

Spatial video data can also be used by researchers to advance our understanding of the spatial process of recovery. In order to achieve this, and likewise to provide community groups with quantifiable outcomes from the video, a method is required to turn images encoded with coordinates into a statistical surface which can be analyzed for patterns. This information would be helpful to answer the question of whether *rebuilding occurs more frequently within “returnee” areas compared to “abandoned” city-blocks?*

As local area analyses of point data are commonly applied in spatial epidemiological investigations, it is useful to borrow for this research techniques

more commonly applied to morbidity and mortality data. For example, local exploration of spatial data could be accomplished by smoothing point level information (usually individual addresses) into continuous rates using a window / filter / kernel (filter from this point on). This technique makes it possible for spatial patterns to be identified without the artificial breaks imposed by choropleth mapping of political units. In a fine-scale recovery example, a smoothed rate surface would show abandonment or return changes within a neighborhood, and not just between neighborhoods.

There are several spatial models or methods of smoothing which can be applied to parcel / property level data (Fotheringham 1997; Fotheringham 1998; Ozdenerol et al. 2005; Wheeler 2007; Grady and Enander 2009). Kernel density smoothing has previously been used on different spatial video surfaces for various neighborhoods of New Orleans, and the results were visualized as contours or as inverted floating clouds (Curtis et al. 2009). Though visually arresting, these surfaces do not offer the same degree of explanatory or investigative potential as DMAP (Disease Mapping and Analysis Program) software (Rushton et al. 1997), a model which has successfully been applied to find local area patterns in infant mortality and cancer data (Rushton and Lolonis 1996; Rushton et al. 2004).

Methods

In order to be able to apply local area analysis techniques to spatial video data, we must first be able to turn the visual information into a quantifiable score for each location. Initial mapping of the spatial video data for neighborhoods of New Orleans employed a 10-point scale of damage assessment (an example can be seen in McCarthy et al. 2008). Although this provides a detailed description of the visual condition of a building, it was found that the variation between people encoding data meant a simpler categorization was required. As a result, a four-point scale was developed and validated for the encoding of recovery data. Under the new attribute extraction scheme, each building is assigned a score of 1, 2, 3, or 4, where 1 = visibly abandoned, 2 = cleared lot, 3 = visibly rebuilding, and 4 = returned. These four categories capture the important elements of a fine-scale “recovering neighborhood,” i.e., properties which have not been returned to or which do not show any sign of return; parcels where some additional action

of the resident has occurred, resulting in the demolition of the property; parcels where the action of return is displayed (these should also correspond to building permits, or rather a subsection of permits where the intention is acted on); and returnees. Using this simple scale, multiple-time periods can also be cross-compared for the same neighborhood to identify locational changes in category (abandoned to rebuilding, rebuilding to returnee, possibly even returnee to re-abandoned).

Category 1 is further subdivided into three sub-categories (2, 5 and 10), where 2 = abandoned but no visible signs of disrepair, 5 = obvious signs of abandonment (for example, broken / boarded windows), and 10 = extreme signs of abandonment (for example, broken windows, a collapsed roof, and severe vegetation overgrowth). Although there is a continuum between 5 and 10, testing and cross-comparison between different encoders found that the distinction between these two categories had a high degree of consistency.

Figure 2 provides examples for each category from a June 2009 data collection trip to New Orleans. Images “A” to “E” would all have initially been encoded as “1,” meaning they were not occupied. However, in the second sub-categorization, “A” would have scored “2” because it looks completely rebuilt and habitable, but there is no obvious evidence of a returnee family. Images “B” and “C” would have scored a “5” because both show visible damage, search and rescue markings, and boarded windows. They do not approach the levels of damage for “D” or “E” which would have scored a “10”. Images “F” and “G” show clear evidence of rebuilding (with work teams visible) and, therefore, they would have scored “3”. Image “H” implies the presence of a returnee and would thus score a “4”—one piece of compelling evidence of occupancy are the manicured flower beds.

In order to spatially explore these data, we have to translate the video into an attribute score per property and assign this value to a single coordinate. One approach is to digitize building outlines from a high resolution aerial photograph, and add the property score to the attribute table of each polygon before placing a point within the polygon. This point is linked to the attribute table. A methodological consideration is, should the point be each building center or should it be a measure of how many families live in each structure, represented by a point on a front door? In Louisiana, one common architectural style is the “shotgun house,” a single-floor structure split along its length into two homes. To what degree

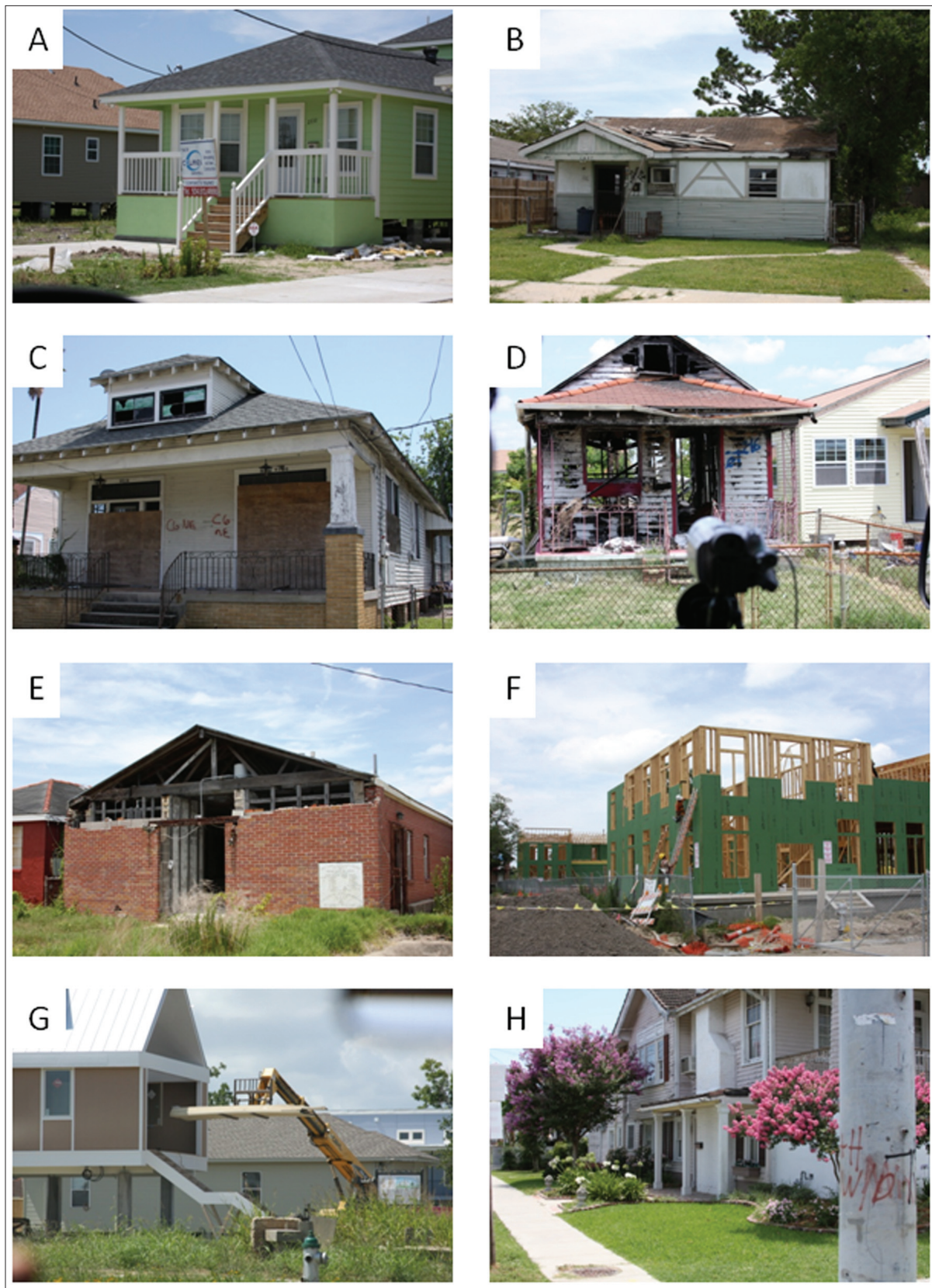


Figure 2. Examples of the visual recovery scale.

will our final hotspot surface change for this type of a home, given the two different inputs? Front-door data are more representative of the number of families affected, but in terms of visual stressors, does a damaged partitioned building have a greater value than a single structure?

A second methodological question is what should the correct filter size be? In general, the larger the filter, the smoother the surface (reducing variability from the data), but also revealing less local detail (Silverman 1978; Rushton et al. 2004). One solution is to use adaptive filters which let data density drive the spatial extent. For this paper, however, two underlying geographic rationales were employed based on the neighborhood under investigation. The first of these covered the average block face (the homes on both sides of the same street segment, approximately 50 m), and the second covered each block and its associated block faces (approximately 100 m) (see Figure 3). Work with the community groups had established that patterns of spatial recovery often manifest themselves at this scale, with the actions of immediate neighbors being important on the decision to return and rebuild, or even to re-abandon. Again, the question asked is, “To what degree will our final hotspot surface change given these variations in filter size?” To sum up, in order to spatially explore the neighborhood recovery surface using spatial video data, attributes are extracted into a GIS using a four-point categorization scheme. The attributes are assigned to two different building points, and for two different scales (filter sizes) of analysis.

As previously mentioned, the model chosen for identifying spatial patterns of recovery in Holy Cross was DMAP (Rushton and Lolonis 1996). The basic premise of DMAP is a grid imposed over the study area, then a filter is placed on every grid node and a rate is calculated within each. As long as the filter radius is greater than half the distance between nodes (and it usually far exceeds this), the rate calculated for each filter will involve points used in multiple rate calculations. As a result, the locations of numerator (for example returnee homes) and denominator (for example all homes) points create a smooth surface rather than one truncated by political boundaries.

In general, the larger the radius of the filter, the more points are included in the rate calculation and the smoother (and less volatile) the final surface tends to be. The output from DMAP consists of a grid with a rate calculation attached to each

node. Under normal epidemiological investigations a second part of the analysis involves a Monte Carlo simulation to assess the significance of these rates—in effect the probability of each denominator becoming a numerator is used to create a simulated rate surface (Rushton et al. 2004). In this respect, recovery data differ from the search for disease hotspots as it is the overall rate pattern that interests us.

Although spatial video data has been collected for several neighborhoods of New Orleans, for the purposes of this paper, Google Street View (GSV)ⁱ was chosen as an information source. The video information from both sources is similar, although there are some physical differences such as GSV offering a broader field of vision while spatial video has higher-resolution imagery. However, these differences are not notable enough to affect the methodology presented in this paper, and as a result, the reader has the ability to replicate the analyses in other neighborhoods of New Orleans (or other post-disaster landscapes captured by GSV).

The Study

Holy Cross (seen in Figure 1) was chosen as the neighborhood of investigation because it suffered both flooding and other storm damage, had mortalities associated with the storm and its aftermath, and continues to have large sections of abandoned property but has a strong neighborhood association and returnee families. In other words, it typifies a New Orleans neighborhood struggling towards normalcy.

Building footprints were digitized in Arc Map 9.3 from high-resolution aerial photography. GSV matched to each building location was coded using the previously described score system. Each coding score was added into the attribute table for each building in the GIS (see Figure 2).

Coordinates were taken from the corners of the Holy Cross neighborhood to create the input grid for DMAP, with the resolution of the grid being approximately 32 m between nodes. The attributes for each building were spatially joined to two shapefiles—the point representing the centroid of each building and the point representing the front door of each building (see Figure 3). The coordinates of these points were then used to calculate the numerator and denominator inputs for DMAP. Numerators were the total number of buildings reaching a threshold for investigation

ⁱ These data were primarily collected in the Fall of 2007.

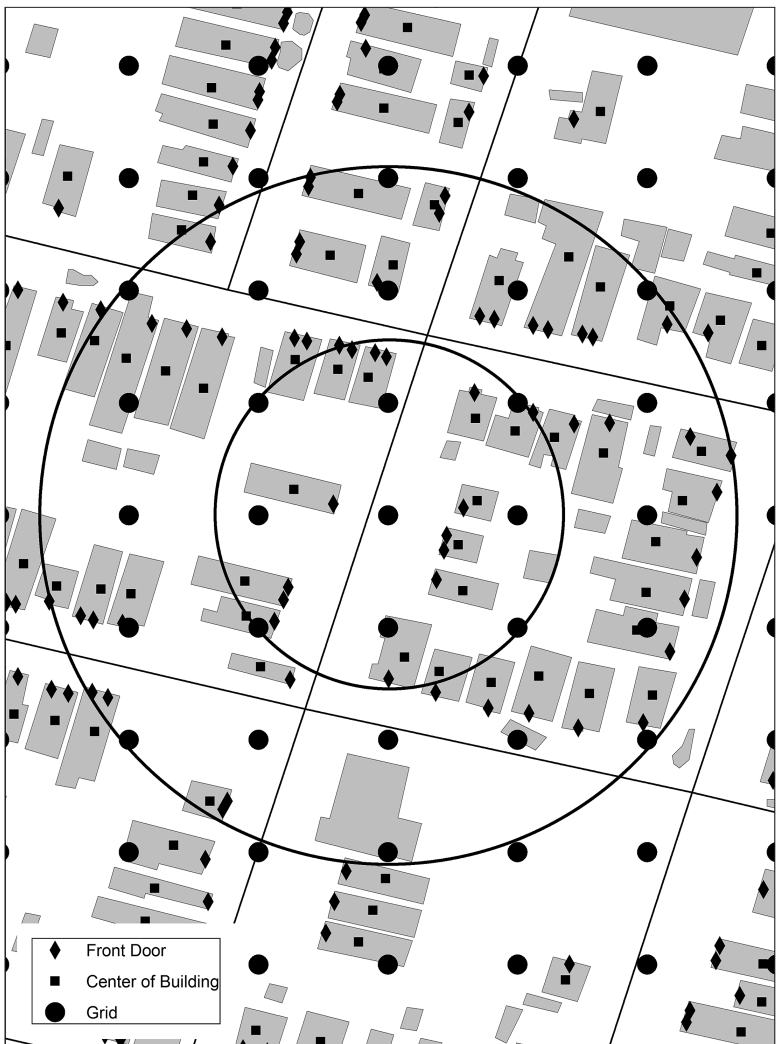


Figure 3. Detail of the spatial choices used in running DMAP. Examples of data points (centroid and front door) to be input into DMAP are shown. The two filter sizes used in the analysis are also displayed. The 50 m filter was selected to cover all homes on one block face. The 100 m filter was selected to cover all homes on a block and each surrounding block face. The overlay between the filter and block did not always coincide for every node, though the two sizes still capture different spatial processes, the immediate neighbors and the wider influencing neighboring area.

(for example, damage is greater than or equal to a score of 5), and the denominator was all “proper” buildings (i.e., excluding sheds, garages, etc).

In order to compare the rate surface for buildings having a damage score of “5” or greater, nodes were selected for each of the four DMAP models (two different point inputs and two different filter sizes) which exceeded the 50 percent and 75 percent level.

This means that for a node to be included in the comparison, more than 50 percent (or 75 percent) of the buildings falling within each DMAP filter had to have a damage score of “5” or greater.

For returnees, the scores of 25 percent and 50 percent were used as thresholds for comparisons, meaning 25 percent (or 50 percent) of all buildings were returned to. The lower thresholds were selected due to the paucity of returnees in the neighborhood. These rates were visualized using contours.

Results

Table 1 shows there were 435 total grid points which were common to each of the four DMAP models, and where 50 percent or more of the total buildings within the filter had a damage score of “5”. Because the total number of grid points for each model type is known too, using the building centroid and a 50 m filter as an example a total of 639 nodes were identified as reaching the 50 percent threshold. Sixty-eight percent of the filter’s total grid points (639) were common to all four models. When the threshold rose to 75 percent of buildings having a damage score of “5” or greater, using the centroid and a 100 m filter produces the best result, with 11 of 19 (or 58 percent) of nodes falling in the combinatory overlay.

When considering returnees at the 50 percent threshold (i.e., 50 percent of all homes within the filter must have been returned to) using the building centroid and a 100 m filter produces the highest proportion of its output

(12 nodes) as being common to all four model types. However, this is only 20 percent of the output, suggesting a high degree of spatial heterogeneity in the data producing considerable variation between models. This is even more apparent when we reduce the threshold to 25 percent, when the proportion of common nodes lies between 42 and 44 percent for each of the four models.

In order to assess how much a single model influenced the combinatory spatial output, the number of common nodes for the remaining three

	50% Buildings Scoring "5"	75% Buildings Scoring "5"	50% Returnees	25% Returnees
Front Door &100m	435 of 826	11 of 118	12 of 73	164 of 382
Centroid & 100m	435 of 775	11 of 19	12 of 60	164 of 381
Front Door & 50m	435 of 668	11 of 230	12 of 140	164 of 372
Centroid & 50m	435 of 639	11 of 185	12 of 119	164 of 366

Table 1. Number of grid points common to each of the four models.

	50% Buildings Scoring "5"	75% Buildings Scoring "5"	50% Returnees	25% Returnees
3 common	50 additional	13 additional	11 additional	23 additional
2 common	225 additional	12 additional	64 additional	130 additional
4 (falling outside)	10	5	0	14
3 (falling outside)	3	0	4	6
2 (falling outside)	69	2	11	73

Table 2. Common nodes for the reduced subset of models, and the number of nodes falling outside of the built area of Holy Cross.

and then two models were calculated. In addition, the number of nodes falling outside of the built environment (especially on the edges) was also recorded.

Table 2 can be interpreted as follows: With a damage score of "5" and a threshold of 50 percent, 50 nodes would be added to the original 435 if only the three remaining models were used (in effect relaxing the analysis by removing the centroid and 50 m filter). If only front door and 100 m and centroid and 100 m were used, the total combined number of nodes rose to 660 (435 + 225).

Table 2 shows that of the 435 nodes common to all four models, and meeting the 50 percent threshold for damage "5", only 10 nodes (about 2 percent) fell outside our area of interest. If the front door and 100 m and centroid and 100 m models were used, the total combined number of nodes would have risen to 660, but as many as 69 (over 10 percent) would have been outside the study area. There is considerable variation across the four different models, and this variation increases based on the

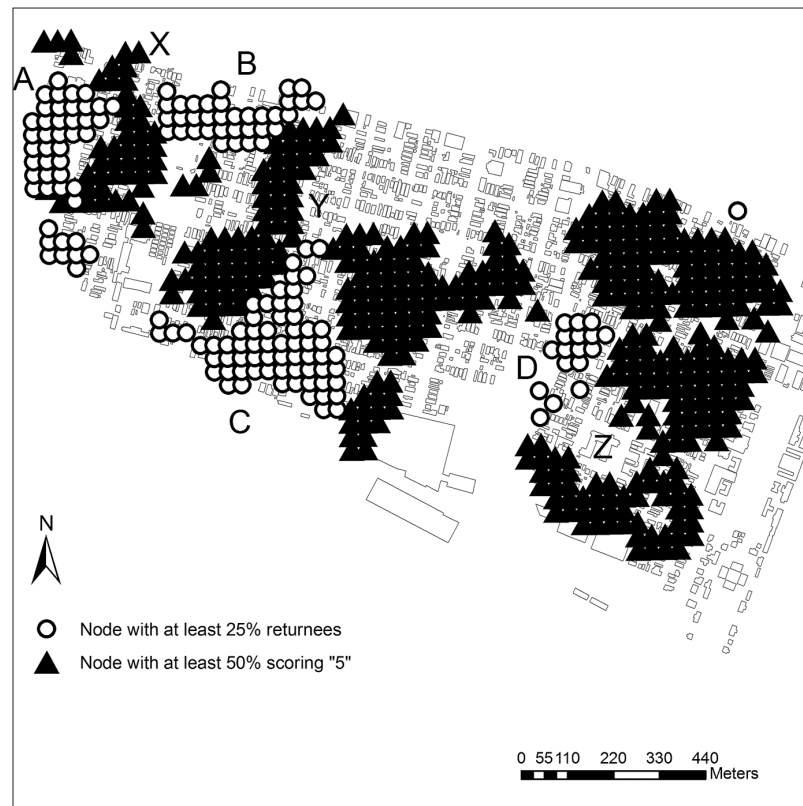


Figure 4. Patterns of recovery and blight in Holy Cross. This map displays the combinatory surfaces of both returnees and visual damage. Four identifiable areas of recovery can be seen on the map, three towards the west (A to B), while a smaller cluster appears to the east (D). The center-left area of recovery (C) might be an area worth further investigation as this also contains the majority of the nodes reaching the 50 percent recovery threshold (not shown on the map).



Figure 5. Detail of the eastern section of Holy Cross. This map shows area Z in Figure 4 and the high concentration of damage there. The map shows each grid point meeting the threshold of 50 percent or greater (meaning at least half the buildings within the filter scored at least “5”). The higher percentages are found in the south western and north eastern section of the map. The map also identifies returnees, including the small returnee cluster seen in (D).

degree of spatial heterogeneity in the original data. However, when all four models are combined to reveal the shared pattern, a conservative surface is generated that reveals spatial trends in abandonment and recovery that can be used for further investigation. Simply put, there are sections of Holy Cross where recovery appears to be occurring, while other sections remain stagnant.

Figure 4 shows that areas with 5 percent and more damage occupy a large portion of the neighbor-

hood not falling in the recovery areas. Indeed, only three nodes share both 50 percent of homes scoring at least “5” damage and having 25 percent of homes being returned to (bottom of Figure 4 A). It is evident that the eastern side of Holy Cross (Z in Figure 4) appears to be in a worse general condition, with the entire area reaching the 50 percent threshold, except for one small section of recovery (D in Figure 4).

Figure 4 also shows that for some sections of the map, recovery and blight are near to each other, especially in the east (A, B and X; C and Y Areas mapped in Figure 4 are displayed in more detail in Figures 5 and 6. These two additional maps show sections dominated by blight (Figure 5) and recovery (Figure 6).

Conclusion

Recovery from the effects of a disaster can be a prolonged process creating various concerns, not least being the loss of culture and community, and the exacerbation of health disparities (Bullard and Wright 2009). Although having effective recovery plans in place before a disaster strikes is important, it can be argued that, not until we understand

how a neighborhood will recover, the pre-event planning process will be limited. A wide array of external influences affects recovery, but in this paper we focused on the finest of scales and how successes and impediments might be revealed as patterns on the landscape—just as other health investigations have begun to combine behavioral, built environment, and social linkages *at the finest of scales* in explaining health dispari-

ties (Kawachi and Berkman 2000). This developing research relies on new, mobile forms of spatial data collection which remove our reliance on large census aggregations and secondary data in general. In this paper, we used the output from GSV (a proxy for spatial video data) to show how these data can be explored for identifying spatial patterns in recovery. This type of spatial analysis can help frame research questions such as why certain streets lag behind, or, is there a diffusion process of returnees? A combinatorial overlay approach of output produces spatial surfaces that, albeit conservative, can be used to identify sections of Holy Cross where recovery and continuing blight are concentrated.

Returning again to Figure 4, it would be interesting to see if recovery diffuses more quickly into blighted areas proximate to recovering sections. For example, will Y recover faster than Z because of the connections to B and C? One benefit of using DMAP is that the output of grid points can be used to show spatial subtleties within each concentration as we attempt to answer these questions. For example, each node can be queried for the percentage of homes that have been returned to, or the percentage of homes with a damage score of "5" or greater, within 50 or 100 m (the two filter radii). By performing the same analysis in a subsequent time period, it would be easy to compare the scores for each node, and therefore quantify change in either direction. A question for future research might be do the nodes to the north of recovery area "C" still meet the same 50 percent threshold, and how much have these rates changed?

Grids facilitate other fine-scale data overlays. For example, spatial regression can be used to explain patterns in the recovering landscape, based on the scores of the closest nodes linked to other data from the period of the storm (mortality locations, 911 calls, flood heights on homes), or more recent surfaces known to act as an impediment

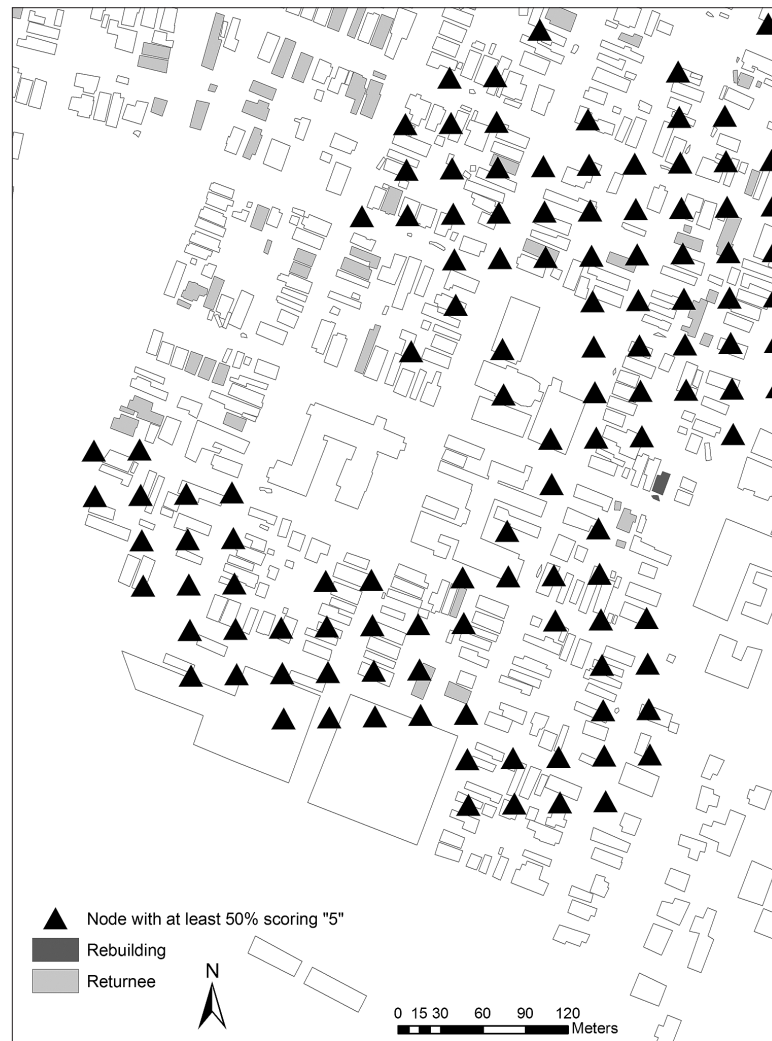


Figure 6. Detail of recovery for one section of Holy Cross. This map focuses on the main recovery area at the bottom center of Figure 4 (C). What is interesting about this pattern is that recovery and blight appear to occupy two distinct sections of the map. However on closer inspection the top right section of the map is a mix of both heavy blight (indicated by the nodes) and returnees. This would certainly be an area of Holy Cross to watch on subsequent data collection trips to see how recovery progresses, and in what pattern.

to recovery, such as crime locations. Figures 5 and 6 also display the degree of spatial heterogeneity present within the neighborhood. In both maps, a returnee's home can be found next to an abandoned property scoring at least "5". What are the implications in terms of day-to-day living experiences for this returnee? Other questions for future research might be: "Did the experience of suffering through Katrina (proxies are 911 calls) result in higher abandonment scores?" or, "Is there a spatial pattern between returnees, blight and crime (victims and places for concealment)?" And returning to one of the main factors

leading to the use of spatial video, “Can patterns in abandonment be linked to postdisaster health problems, especially psychopathology?” In addition, a question that can only be answered using a spatial video, “How do these patterns change over time?”

ACKNOWLEDGMENTS

The authors would like to thank the University Southern California for undergraduate SURF funding, and Advancing Scholarship in the Humanities and Social Sciences funding, our undergraduates who have visited New Orleans on data collection trips, and our community collaborators, especially Donald Butte and Julius Lee. We would also like to thank the reviewers of the paper for their insightful comments.

REFERENCES

- Alesh, D.J., L.A. Arendt, and J.N. Holly. 2009. *Managing for long-term community recovery in the aftermath of disaster*. Public Entity Risk Institute, Fairfax, Virginia.
- Bullard, R.D., and B. Wright. 2009. *Race, place and environmental justice after Hurricane Katrina*. Boulder, CO Westview Press.
- Cefalu, W.T., S.R. Smith, L. Blonde, and V. Fonseca. 2006. The Hurricane Katrina aftermath and its impact on diabetes care: Observations from “ground zero”: Lessons in disaster preparedness of people with diabetes. *Diabetes Care* 29: 158-60.
- Comerio, M.C. 1998. *Disaster hits home: New policy for urban housing recovery*. Berkeley, California: University of California Press.
- Curtis, A., J.W. Mills, T. McCarthy, A.S. Fotheringham, and W.F. Fagan. 2009. Space and time changes in neighborhood recovery after a disaster using a spatial video acquisition system. In: P. Showalter and L. Yongmei (eds), *Contributions to urban hazard and disaster analysis*. Springer 373-394.
- Curtis, A. 2008. From healthy start to Hurricane Katrina: Using GIS to eliminate disparities in perinatal health. *Statistics in Medicine* 27(20): 3984-97.
- Curtis, A., J. Mills, B. Kennedy, S. Fotheringham, and T. McCarthy. 2007. Understanding the geography of post-traumatic stress: An academic justification for using a spatial video acquisition system in the response to Hurricane Katrina. *Journal of Contingencies and Crisis Management* 15(4): 208-19.
- Duval-Diop, D., A. Curtis, and A. Clark. 2010. Enhancing equity with public participatory GIS in hurricane rebuilding: Faith based organizations, community mapping, and policy advocacy. *Journal of the Community Development Society* 41(1): Duval-Diop, D., and K. Rose. 2008. *Delivering equitable development to a recovering Louisiana: A state policy guide for 2008 and beyond*. New Orleans, Louisiana: PolicyLink.
- Fotheringham, A.S. 1997. Trends in quantitative methods I: Stressing the local. *Progress in Human Geography* 21: 88-96.
- Fotheringham, A.S. 1998. Trends in quantitative methods II: Stressing the computational. *Progress in Human Geography* 22(2): 283-92.
- Grady, S.C., and H. Enander. 2009. Geographic analysis of low birthweight and infant mortality in Michigan using automated zoning methodology. *International Journal of Health Geographics* 8: 10.
- Grubesic, T H, T. C.Matisziw and C Timothy. 2006. On the use of ZIP codes and ZIP code tabulation areas (ZCTAs) for the spatial analysis of epidemiological data *International Journal of Health Geographics* 5: 58.
- Haas, J.E., R.W. Kates, and M.J. Bowden. 1977. *Reconstruction following disaster*. Cambridge, Massachusetts: MIT Press.
- Hartman, C., and G. Squires (eds). 2006. There is no such thing as a natural disaster: Race, class and Hurricane Katrina. New York, New York: Routledge.
- Holzer, H.J., and R.I. Lerman. 2006. *Employment issues and challenges in post-Katrina New Orleans*. The Urban Institute.
- Kawachi, I., and L. Berkman. 2000. *Neighborhoods and health*. Oxford University Press. Oxford New York
- Kunreuther, H. 2006. Disaster mitigation and insurance: Learning from Katrina. *Annals of the American Academy of Political and Social Science* 604: 208-27.
- Liu, A., and A. Plyer. 2008. The New Orleans index anniversary edition: Three years after Katrina. [<http://www.brookings.edu/reports/2007/08neworleansindex.aspx>; accessed July 11, 2009].
- McCarthy, T., R. Farrell, A. Curtis, and A.S. Fotheringham. 2008. Integrated remotely sensed datasets for disaster management. *SPIE Europe Proceedings*, Vol 7110 Cardiff
- Madrid, P.A., R. Grant, M.J. Reilly, and N.B. Redlener. 2006. Challenges in meeting immediate emotional needs: Short-term impact of a major disaster on children's mental health: Building resiliency in the aftermath of Hurricane Katrina. *Pediatrics* 117: S448-53.
- Mills, J. 2008. Understanding disaster: GI Science contributions in the ongoing recovery from Katrina. *Transactions in GIS* 12(1): 1-4.
- Mills, J.W., A. Curtis, J. Pine, B. Kennedy, F. Jones, R. Ramani, and D. Bausch. 2008. The clearinghouse concept: A model for geospatial data centralization and dissemination in a disaster. *Disasters* 32(3): 467-79.
- Ozdenerol, E., B.L. Williams, S.Y. Kang, and M.S. Magsumbol. 2005. Comparison of spatial scan statistic and spatial filtering in estimating low birth weight clusters. *International Journal of Health Geographics* 4: 19.

- Penner, D.R., and K.C. Ferdinand. 2009. Overcoming Katrina: African American voices from the Crescent City and beyond Palgrave. New York, New York: Macmillan.
- Petersen, D., M. Minkler, V. Breckwich Vásquez, and A.C. Baden. 2006. Community-based participatory research as a tool for policy change: A case study of the Southern California Environmental Justice Collaborative. *Review of Policy Research* 23(2): 339-354.
- Richards, L., and M. Dalbey. 2006. Creating great places: The role of citizen participation. *Journal of the Community Development Society* 37(4): 18-32.
- Rushton, G., and P. Lolonis. 1996. Exploratory spatial analysis of birth defect rates in an urban population. *Statistics in Medicine* 15: 717-26.
- Rushton, G., M.P. Armstrong, C. Lynch, and J. Rohrer. 1997. Improving public health through Geographical Information Systems: An instructional guide to major concepts and their implementation. Iowa City, Iowa: The University of Iowa, Department of Geography.
- Rushton, G., I. Peleg, A. Banerjee, G. Smith, and M. West. 2004. Analyzing geographic patterns of disease incidence: Rates of late-stage colorectal cancer in Iowa. *Journal of Medical Systems* 28(3): 224-36.
- Sampson, J., and S.W. Raudenbush. 1999. Systematic social observation of public spaces: A new look at disorder in urban neighborhoods. *American Journal of Sociology* 105(3): 603-51.
- Silverman, B.W. 1978. Choosing the window width when estimating a density. *Biometrika* 65: 1-11.
- Vale, L.J. and T.J. Campanella 2005 *The resilient city: how modern cities recover from disaster*, Oxford University Press, New York
- Wheeler, D.C. 2007. A comparison of spatial clustering and cluster detection techniques for childhood leukemia incidence in Ohio, 1996-2003. *International Journal of Health Geographics* 6: 13.
- Wright, J.D., P.H. Rossi, S.R. Wright, and E. Weber-Burton. 1979. *After the clean-up: Long-range effects of natural disasters*. Beverly Hills, California: Sage Publications.